Measurement of the Atmospheric ν_e flux in IceCube

M. G. Aartsen,[2] R. Abbasi,[27] Y. Abdou,[22] M. Ackermann,[41] J. Adams,[15] J. A. Aguilar,[21] M. Ahlers,[27] D. Altmann,[9] J. Auffenberg,[27] X. Bai,[31,*] M. Baker,[27] S. W. Barwick,[23] V. Baum,[28] R. Bay,[7] K. Beattie,[8] J. J. Beatty,[17,18] S. Bechet,[12] J. Becker Tjus,[10] K.-H. Becker,[40] M. Bell,[38] M. L. Benabderrahmane,[41] S. BenZvi,[27] J. Berdermann,[41] P. Berghaus,[41] D. Berley,[16] E. Bernardini,[41] A. Bernhard,[30] D. Bertrand,[12] D. Z. Besson,[25] D. Bindig,[40] M. Bissok,[1] E. Blaufuss,[16] J. Blumenthal,[1] D. J. Boersma,[39,1] S. Bohaichuk,[20] C. Bohm,[34] D. Bose,[13] S. Böser,[11] O. Botner,[39] L. Brayeur,[13] A. M. Brown,[15] R. Bruijn,[24] J. Brunner,[41] S. Buitink,[13] M. Carson,[22] J. Casey,[5] M. Casier,[13] D. Chirkin,[27] B. Christy,[16] K. Clark,[38] F. Clevermann,[19] S. Cohen,[24] D. F. Cowen,[38,37] A. H. Cruz Silva,[41] M. Danninger,[34] J. Daughhetee,[5] J. C. Davis,[17] C. De Clercq,[13] S. De Ridder,[22] P. Desiati,[27] G. de Vries-Uiterweerd,[22] M. de With,[9] T. DeYoung,[38,†] J. C. Díaz-Vélez,[27] J. Dreyer,[10] M. Dunkman,[38] R. Eagan,[38] B. Eberhardt,[28] J. Eisch,[27] R. W. Ellsworth,[16] O. Engdegård,[39] S. Euler,[1] P. A. Evenson,[31] O. Fadiran,[27] A. R. Fazely,[6] A. Fedynitch,[10] J. Feintzeig,[27] T. Feusels,[22] K. Filimonov,[7] C. Finley,[34] T. Fischer-Wasels,[40] S. Flis,[34] A. Franckowiak,[11] R. Franke,[41] K. Frantzen,[19] T. Fuchs,[19] T. K. Gaisser,[31] J. Gallagher,[26] L. Gerhardt,[8,7] L. Gladstone,[27] T. Glüsenkamp,[41] A. Goldschmidt,[8] G. Golup,[13] J. A. Goodman,[16] D. Góra,[41] D. Grant,[20] A. Groß,[30] M. Gurtner,[40] C. Ha,[8,7,†] A. Haj Ismail,[22] A. Hallgren,[39] F. Halzen,[27] K. Hanson,[12] D. Heereman,[12] P. Heimann,[1] D. Heinen,[1] K. Helbing,[40] R. Hellauer,[16] S. Hickford,[15] G. C. Hill,[2] K. D. Hoffman,[16] R. Hoffmann,[40] A. Homeier,[11] K. Hoshina,[27] W. Huelsnitz,[16,‡] P. O. Hulth,[34] K. Hultqvist,[34] S. Hussain,[31] A. Ishihara,[14] E. Jacobi,[41] J. Jacobsen,[27] G. S. Japaridze,[4] K. Jero,[27] O. Jlelati,[22] B. Kaminsky,[41] A. Kappes,[9] T. Karg,[41] A. Karle,[27] J. L. Kelley,[27] J. Kiryluk,[35] F. Kislat,[41] J. Kläs,[40] S. R. Klein,[8,7] J.-H. Köhne,[19] G. Kohnen,[29] H. Kolanoski,[9] L. Köpke,[28] C. Kopper,[27] S. Kopper,[40] D. J. Koskinen,[38] M. Kowalski,[11] M. Krasberg,[27] G. Kroll,[28] J. Kunnen,[13] N. Kurahashi,[27] T. Kuwabara,[31] M. Labare,[13] H. Landsman,[27] M. J. Larson,[36] M. Lesiak-Bzdak,[35] J. Leute,[30] J. Lünemann,[28] J. Madsen,[33] R. Maruyama,[27] K. Mase,[14] H. S. Matis,[8] F. McNally,[27] K. Meagher,[16] M. Merck,[27] P. Mészáros,[37,38] T. Meures,[12] S. Miarecki,[8,7] E. Middell,[41] N. Milke,[19] J. Miller,[13] L. Mohrmann,[41] T. Montaruli,[21,§] R. Morse,[27] R. Nahnhauer,[41] U. Naumann,[40] H. Niederhausen,[35] S. C. Nowicki,[20] D. R. Nygren,[8] A. Obertacke,[40] S. Odrowski,[30] A. Olivas,[16] M. Olivo,[10] A. O'Murchadha,[12] S. Panknin,[11] L. Paul,[1] J. A. Pepper,[36] C. Pérez de los Heros,[39] C. Pfendner,[17] D. Pieloth,[19] N. Pirk,[41] J. Posselt,[40] P. B. Price,[7] G. T. Przybylski,[8] L. Rädel,[1] K. Rawlins,[3] P. Redl,[16] E. Resconi,[30] W. Rhode,[19] M. Ribordy,[24] M. Richman,[16] B. Riedel,[27] J. P. Rodrigues,[27] C. Rott,[17] T. Ruhe,[19] B. Ruzybayev,[31] D. Ryckbosch,[22] S. M. Saba,[10] T. Salameh,[38] H.-G. Sander,[28] M. Santander,[27] S. Sarkar,[32] K. Schatto,[28] M. Scheel,[1] F. Scheriau,[19] T. Schmidt,[16] M. Schmitz,[19] S. Schoenen,[1] S. Schöneberg,[10] L. Schönherr,[1] A. Schönwald,[41] A. Schukraft,[1] L. Schulte,[11] O. Schulz,[30] D. Seckel,[31] S. H. Seo,[34] Y. Sestayo,[30] S. Seunarine,[33] C. Sheremata,[20] M. W. E. Smith,[38] M. Soiron,[1] D. Soldin,[40] G. M. Spiczak,[33] C. Spiering,[41] M. Stamatikos,[17,¶] T. Stanev,[31] A. Stasik,[11] T. Stezelberger,[8] R. G. Stokstad,[8] A. Stößl,[41] E. A. Strahler,[13] R. Ström,[39] G. W. Sullivan,[16] H. Taavola,[39] I. Taboada,[5] A. Tamburro,[31] S. Ter-Antonyan,[6] S. Tilav,[31] P. A. Toale,[36] S. Toscano,[27] M. Usner,[11] D. van der Drift,[8,7] N. van Eijndhoven,[13] A. Van Overloop,[22] J. van Santen,[27] M. Vehring,[1] M. Voge,[11] M. Vraeghe,[22] C. Walck,[34] T. Waldenmaier,[9] M. Wallraff,[1] R. Wasserman,[38] Ch. Weaver,[27] M. Wellons,[27] C. Wendt,[27] S. Westerhoff,[27] N. Whitehorn,[27] K. Wiebe,[28] C. H. Wiebusch,[1] D. R. Williams,[36] H. Wissing,[16] M. Wolf,[34] T. R. Wood,[20] K. Woschnagg,[7] C. Xu,[31] D. L. Xu,[36] X. W. Xu,[6] J. P. Yanez,[41] G. Yodh,[23] S. Yoshida,[14] P. Zarzhitsky,[36] J. Ziemann,[19] S. Zierke,[1] A. Zilles,[1] and M. Zoll[34]

(IceCube Collaboration)

[1] *III. Physikalisches Institut, RWTH Aachen University, D-52056 Aachen, Germany*
[2] *School of Chemistry & Physics, University of Adelaide, Adelaide SA, 5005 Australia*
[3] *Dept. of Physics and Astronomy, University of Alaska Anchorage, 3211 Providence Dr., Anchorage, AK 99508, USA*
[4] *CTSPS, Clark-Atlanta University, Atlanta, GA 30314, USA*
[5] *School of Physics and Center for Relativistic Astrophysics, Georgia Institute of Technology, Atlanta, GA 30332, USA*
[6] *Dept. of Physics, Southern University, Baton Rouge, LA 70813, USA*
[7] *Dept. of Physics, University of California, Berkeley, CA 94720, USA*
[8] *Lawrence Berkeley National Laboratory, Berkeley, CA 94720, USA*
[9] *Institut für Physik, Humboldt-Universität zu Berlin, D-12489 Berlin, Germany*
[10] *Fakultät für Physik & Astronomie, Ruhr-Universität Bochum, D-44780 Bochum, Germany*
[11] *Physikalisches Institut, Universität Bonn, Nussallee 12, D-53115 Bonn, Germany*

[12] *Université Libre de Bruxelles, Science Faculty CP230, B-1050 Brussels, Belgium*
[13] *Vrije Universiteit Brussel, Dienst ELEM, B-1050 Brussels, Belgium*
[14] *Dept. of Physics, Chiba University, Chiba 263-8522, Japan*
[15] *Dept. of Physics and Astronomy, University of Canterbury, Private Bag 4800, Christchurch, New Zealand*
[16] *Dept. of Physics, University of Maryland, College Park, MD 20742, USA*
[17] *Dept. of Physics and Center for Cosmology and Astro-Particle Physics, Ohio State University, Columbus, OH 43210, USA*
[18] *Dept. of Astronomy, Ohio State University, Columbus, OH 43210, USA*
[19] *Dept. of Physics, TU Dortmund University, D-44221 Dortmund, Germany*
[20] *Dept. of Physics, University of Alberta, Edmonton, Alberta, Canada T6G 2G7*
[21] *Département de physique nucléaire et corpusculaire, Université de Genève, CH-1211 Genève, Switzerland*
[22] *Dept. of Physics and Astronomy, University of Gent, B-9000 Gent, Belgium*
[23] *Dept. of Physics and Astronomy, University of California, Irvine, CA 92697, USA*
[24] *Laboratory for High Energy Physics, École Polytechnique Fédérale, CH-1015 Lausanne, Switzerland*
[25] *Dept. of Physics and Astronomy, University of Kansas, Lawrence, KS 66045, USA*
[26] *Dept. of Astronomy, University of Wisconsin, Madison, WI 53706, USA*
[27] *Dept. of Physics and Wisconsin IceCube Particle Astrophysics Center, University of Wisconsin, Madison, WI 53706, USA*
[28] *Institute of Physics, University of Mainz, Staudinger Weg 7, D-55099 Mainz, Germany*
[29] *Université de Mons, 7000 Mons, Belgium*
[30] *T.U. Munich, D-85748 Garching, Germany*
[31] *Bartol Research Institute and Department of Physics and Astronomy, University of Delaware, Newark, DE 19716, USA*
[32] *Dept. of Physics, University of Oxford, 1 Keble Road, Oxford OX1 3NP, UK*
[33] *Dept. of Physics, University of Wisconsin, River Falls, WI 54022, USA*
[34] *Oskar Klein Centre and Dept. of Physics, Stockholm University, SE-10691 Stockholm, Sweden*
[35] *Department of Physics and Astronomy, Stony Brook University, Stony Brook, NY 11794-3800, USA*
[36] *Dept. of Physics and Astronomy, University of Alabama, Tuscaloosa, AL 35487, USA*
[37] *Dept. of Astronomy and Astrophysics, Pennsylvania State University, University Park, PA 16802, USA*
[38] *Dept. of Physics, Pennsylvania State University, University Park, PA 16802, USA*
[39] *Dept. of Physics and Astronomy, Uppsala University, Box 516, S-75120 Uppsala, Sweden*
[40] *Dept. of Physics, University of Wuppertal, D-42119 Wuppertal, Germany*
[41] *DESY, D-15735 Zeuthen, Germany*

(Dated: March 25, 2013)

We report the first measurement of the atmospheric electron neutrino flux in the energy range between approximately 80 GeV and 6 TeV, using data recorded during the first year of operation of IceCube's DeepCore low energy extension. Techniques to identify neutrinos interacting within the DeepCore volume and veto muons originating outside the detector are demonstrated. A sample of 1029 events is observed in 281 days of data, of which $496 \pm 66(\text{stat.}) \pm 88(\text{syst.})$ are estimated to be cascade events, including both electron neutrino and neutral current events. The rest of the sample includes residual backgrounds due to atmospheric muons and charged current interactions of atmospheric muon neutrinos. The flux of the atmospheric electron neutrinos is consistent with models of atmospheric neutrinos in this energy range. This constitutes the first observation of electron neutrinos and neutral current interactions in a very large volume neutrino telescope optimized for the TeV energy range.

PACS numbers: 95.55.Vj, 14.60.Lm, 29.40.Ka, 95.85.Ry, 25.30.Pt

The atmospheric ν_μ spectrum (we do not differentiate between $\overline{\nu}$ and ν) has been measured at energies up to 400 TeV [1]. Much less is known about atmospheric ν_e. These ν_e come mostly from the decays of kaons and muons produced in cosmic-ray air showers. Underground water Cherenkov telescopes like IMB-3 and Super-Kamiokande as well as calorimetric detectors such as Fréjus, NUSEX, and Soudan-2 have studied atmospheric ν_e with energies up to a few tens of GeV [2–6], but no measurement has been made at higher energies. So far, searches for ν_e at higher energies have yielded upper limits [7–10]. Theoretical calculations for atmospheric ν_e are poorly constrained at energies above 100 GeV due to the uncertainties in kaon production [11, 12].

In this Letter, we report on a measurement of atmospheric neutrino-induced cascades using the DeepCore infill array in IceCube. "Cascades" are ν_e charged current (CC) interactions and neutral current (NC) interactions of neutrinos of all flavors. From a selected sample of cascade candidate events, an atmospheric ν_e flux is obtained in the energy range between 80 GeV and 6 TeV.

In addition to their interest for understanding particle production in air showers, the results presented here are a first step toward measurement of the appearance

of ν_τ (which is indistinguishable from ν_e in IceCube at these energies) due to neutrino flavor oscillations [13]. The first oscillation maximum for $\nu_\mu \to \nu_\tau$, and corresponding minimum in the ν_μ survival probability, occurs at 24 GeV for vertically upward-going neutrinos [14], so this measurement of atmospheric ν_e at higher energy is an important baseline for understanding the flux at energies where oscillation effects are unimportant.

IceCube is a high-energy neutrino detector buried in the Antarctic ice. It observes Cherenkov light from neutrino interactions. The main detection signatures for neutrinos are long, straight tracks and approximately spherical cascades. The former are created by neutrino-induced muons while the latter are produced by neutrino-induced electromagnetic and/or hadronic showers. The DeepCore infill array [15] to IceCube reduces the energy threshold of IceCube to energies as low as 10 GeV. DeepCore's denser optical module spacing, higher quantum efficiency photomultiplier tubes, and lower trigger threshold, along with its deployment in the clearest ice, all enhance low-energy neutrino detection.

This analysis used the first IceCube data run with DeepCore, from June 2010 to May 2011 when a total of 79 IceCube strings, including six specialized DeepCore strings, were operational. Each string consists of 60 digital optical modules (DOMs), equipped with a photomultipler tube [16] and data acquisition electronics [17]. The DeepCore fiducial volume included these six strings and the seven adjacent standard IceCube strings. Since then, the remaining seven IceCube strings have been deployed, including two additional DeepCore strings.

The DeepCore fiducial volume contains the 454 DOMs deployed at depths greater than 2100 m on the 13 strings of DeepCore. A dedicated DeepCore trigger [15] was run on these DOMs. It read out the full IceCube detector if photons ("hits") were observed in local coincidence (LC) on at least three neighboring DOMs within 2.5 μs [17]. The average trigger rate was 185 Hz, a factor 13 smaller than the total IceCube trigger rate.

To avoid observational bias, 10% of the data, distributed evenly through the year, were used to develop the analysis and verify the detector simulation. After application of general data quality criteria, the 281 live-days of the remaining 90% of the data set are used for the results presented here.

To observe cascades, one must reject two types of backgrounds which are more numerous than the desired signal. The first class is "atmospheric muons" produced in cosmic-ray air showers in the Earth's atmosphere, which penetrate the 2100 m of ice above DeepCore and produce hits in the fiducial volume. The second class, much less common than the first, consists of atmospheric ν_μ also produced in air showers, which undergo CC interactions in the ice but produce relatively low energy muons, making them difficult to distinguish from cascades. Simulated data are obtained from Monte Carlo (MC) programs modeling the detector response to both of these types of background, as well as neutrino-induced cascades. An extensive air shower simulation [18] is used for atmospheric muons and a separate program [19] is for neutrinos weighted with the Honda [11] and the Bartol [20] atmospheric flux predictions. Selection criteria are applied to the data to reduce these backgrounds sufficiently to observe cascades. Fig. 1 compares the performance of these criteria with the predicted performance.

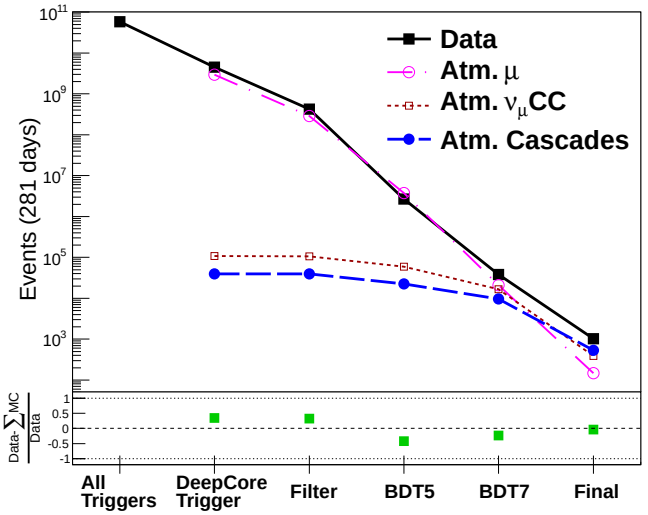

FIG. 1. (Color online) The number of data events (black filled squares) passing each selection criteria is shown with the MC predictions: atmospheric muon (magenta open circles), atmospheric ν_μ CC (red open squares), and cascade signal (blue filled circles). From left to right on the horizontal axis: all triggered events, DeepCore triggered events, DeepCore filtered events, 5-variable BDT cut (BDT5), 7-variable BDT cut(BDT7), and the final selection. Lines are to guide the eye.

The initial background rejection focuses on eliminating atmospheric muons. Following the standard DeepCore trigger, an online veto algorithm [15] rejects events with possible traces of an entering muon seen by the outer strings of the IceCube detector. A secondary trigger is applied in software to remove spurious triggers due to dark noise, requiring at least eight hits in the event, of which at least four must be in the fiducial volume. In contrast to the hardware trigger, both locally-coincident and non-coincident signals which are correlated in time and space with the event are included.

Next, five variables quantifying the event topology are calculated. These are the depth of the first hit in the event, the sphericity of the event (the ratio of the smallest eigenvalue to the sum of all eigenvalues, the analogue of the tensor of inertia obtained by treating each hit as a point mass), the fraction of the total number of photoelectrons which are recorded within the first 600 ns (i.e., a measure of how fast the event develops), a similar fraction calculation excluding the two earliest hits assuming they may be due to noise, and the number of

hits occurring in the veto region regardless of their time or location. These variables are used to train a boosted decision tree (BDT) [21]. A cut on this 5-variable BDT reduces the number of data events to 2.7×10^6, a factor of 1660 reduction from the DeepCore trigger. The number of predicted atmospheric cascades is 2.3×10^4 at this stage.

More computationally intensive event reconstruction algorithms are run over the surviving events, successively reconstructing the events under the hypotheses that they are produced by atmospheric muons or by neutrino-induced cascades. These likelihood-based reconstructions take into account the details of Cherenkov light propagation in the ice [22]. A second BDT is then trained to discriminate between atmospheric muons and cascades, using seven variables: the ratio of the best-fit likelihoods obtained from these reconstructions, the depth of the first hit, the horizontal distance of the first hit from the center of DeepCore, the fraction of the total number of photoelectrons detected within the first 300 ns, and variables measuring whether the hit pattern tends to drift across the detector during the event, indicative of a muon-like track through the detector rather than a spherically expanding light pattern which is a typical signature of a cascade. The numbers of events passing the second BDT are 3.8×10^4 (data), 2.1×10^4 (atm. μ), 1.7×10^4 (atm. ν_μ CC), and 9.6×10^3(atm. cascades).

Following this second BDT, the atmospheric muon rate is reduced sufficiently that the final steps of event selection focus on reducing the background of tracklike neutrino events produced by ν_μ CC interactions rather than the cascades produced by ν_e or ν_μ NC interactions. These are mostly ν_μ CC events interacting within the DeepCore volume. The hadronic cascade produced at the neutrino interaction vertex may obscure the muon track emanating from the vertex unless the muon has sufficient energy to travel a considerable distance and is oriented such that it does not escape the detector volume undetected. To reduce this ν_μ CC background, we apply several additional criteria. We require that the reconstructed neutrino interaction vertex of the event not be near the top or bottom of the DeepCore volume, where a muon track could be missed if it escapes into the uninstrumented ice below the detector or the relatively dusty ice above DeepCore, and that the first hit in the event also fall in this volume. We further require that the best-fit cascade likelihood be both relatively good and also better than that obtained from the track fit, that enough DOMs were hit in the event that the comparison between these fits should have discrimination power, and finally we require a high (signal-like) value from the second, 7-variable BDT [23].

In contrast to the criteria used to reject atmospheric muons, this discrimination against ν_μ CC events leads to significant loss of neutrino cascade events, not only due to the reduced fiducial volume but also because low energy cascades rarely produce enough hits to satisfy the

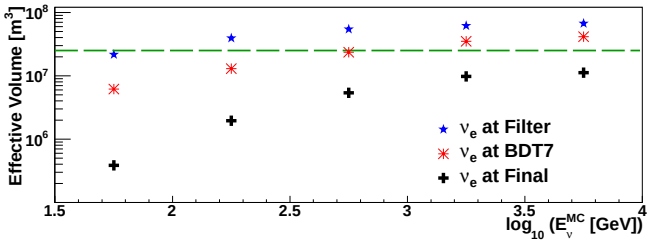

FIG. 2. (Color online) Effective volumes at different cut levels as a function of MC ν_e energy. The green dashed line indicates an instrumented cylinder volume with a height of 200 m and a radius of 200 m.

requirements. The steeply falling atmospheric neutrino spectrum and the very low online trigger threshold mean that the overall efficiency shown in Fig. 1 is dominated by the low energy events, but as shown in Fig. 2, 40% of the cascades within the fiducial volume pass these cuts above 1 TeV.

In total, 1029 events pass all of these criteria. Simulations show that about half of these events are residual backgrounds due to atmospheric muons (14%) and ν_μ CC events (36%). The remainder are ν_e and ν_μ NC events (inseparable from ν_e). The MC predicts that half of the cascades are produced by ν_e (primarily CC interactions) and half are ν_μ NC events. The final event rates are shown in Table I and the effective volumes of ν_e simulation at different selection levels are shown in Fig. 2. For atmospheric muons, the overall rejection is 4×10^8 with respect to the total IceCube trigger rate. These atmospheric muons mimic the cascade signature in the fiducial region by losing most of their energy in a single interaction; they evade the veto cuts by entering the IceCube detector from the side on a relatively steep trajectory (typically around 60° in the zenith angle) in a region where the optical properties of the ice are poorer than average [24, 25], so that in unfortunate cases no Cherenkov photons are detected by the veto. The rarity of these events and the limited size of the simulated atmospheric muon sample which could be produced with the available computational resources results in a large statistical uncertainty in this background, but its importance is clearly secondary to that of the misidentified muon neutrino events.

The largest systematic uncertainty in the signal prediction comes from the light detection efficiency in a DOM *in situ*. The uncertainty in the absolute efficiency of the PMT is measured in a laboratory to be 8% [16] which dominates the DOM sensitivity. Studies of efficiency in situ with atmospheric muon data lead to an estimated 10% uncertainty in the DOM sensitivity when local effects in the refrozen ice are included. Varying the efficiency by 10% in the simulations, the predicted atmospheric neutrino rate changes by 11% for ν_μ and 10% for ν_e. The same procedure is performed for the atmospheric muons, except at an earlier stage (BDT7) of the analysis to ensure adequate statistics and gives 30% uncertainty.

TABLE I. The number of events in 281 days are shown after application of all selection criteria. N^{obs} denotes the number of observed data events. An average of the Bartol and Honda event rates is also shown. The neutrino simulations have statistical uncertainties of less than 2% while the atmospheric muon MC has a statistical uncertainty of 45%.

	Signal			Background		MC	N^{obs}
Type	ν_eNC	ν_eCC	ν_μNC	ν_μCC	atm. μ	Sum	
Bartol	26	290	267	403	147	1134	-
Honda	19	227	245	368	147	1007	-
Average	23	259	256	385	147	1070	-
Data	-	-	-	-	-	-	1029

TABLE II. Systematic uncertainties.

Source of uncertainties	atm. μ	atm. ν_μ	atm. ν_e
Ice properties	8%	6%	2%
DOM efficiency	30%	11%	10%
Cosmic-ray flux	33%	-	-
ν-nucleon cross section	-	6%	6%
Sum	45%	14%	11%

The systematic uncertainties due to the optical properties of ice are estimated as 8% for atmospheric muons and 6% (2%) for atmospheric ν_μ (ν_e) by comparing final level rates from simulations with two different ice models. The optical properties of the ice are determined from measurements using calibration light source data in the DOMs [24, 25].

We conservatively estimate the uncertainty in the atmospheric muon rate due to uncertainties in cosmic ray composition by comparing our baseline simulation, based on spectra of individual elements [26] with a proton-only composition model. The comparison is made at the BDT7 stage to ensure sufficient statistics, and shows a rate variation of 25%. Additionally, a 20% uncertainty for the cosmic ray flux normalization and 6% for the seasonal rate variation are included. These are summed in quadrature and give a total of 33% cosmic-ray flux uncertainty. Though large, this cosmic-ray flux uncertainty is smaller than the statistical uncertainty in the atmospheric muon rate due to the limited MC sample, so we use this estimate as the systematic uncertainty. The systematic uncertainty for neutrino-nucleon cross sections is estimated to be 6%. The atmospheric ν_μ flux uncertainties of 9% are obtained by comparing the final event rates with the Honda and Bartol flux predictions. Neutrino oscillations have a very small effect in this sample (1.8% for ν_μ and 0.1% for ν_e). The ν_τ contribution is estimated to be less than 1% of the data sample assuming standard oscillation parameters [27]. The total systematic uncertainties are 14% (11%) for atmospheric ν_μ (ν_e) and 45% for atmospheric muons, as shown in Table II.

The atmospheric muon background and the atmospheric ν_μ CC background are subtracted from the data. The latter contribution is estimated by averaging the Bartol and Honda atmospheric neutrino predictions. Half the difference is included in the systematic uncertainties. We observe an excess of cascade events,

$$N_{\rm cascade} = 496 \pm 66(\text{stat.}) \pm 88(\text{syst.}) \ ,$$

where the total statistical uncertainty includes statistical uncertainties of the two subtracted background components, and the total systematic uncertainty is a sum in quadrature of the ν_μ CC systematic uncertainties and the atmospheric muon systematic uncertainties. Since part of the systematic uncertainties does not come from the final level comparison, we conservatively do not consider the correlations among the systematic uncertainties. The cascade signal has a significance of 4.5 σ. We estimate based on simulations that 240 $\pm$ 66(stat.) $\pm$ 109(syst.) of the cascades are produced by ν_e. The data are in good agreement with the Honda model, and slightly below (though still consistent with) the Bartol model which predicts 127 more neutrino events in total.

The lower rate prediction from the Honda model, especially in ν_e, is due to the different treatment of kaon production in the atmosphere [28], and is shown in Table I. Both Honda and Bartol estimate roughly 15% uncertainties in the atmospheric ν_e flux at 100 GeV rising to 25% at 1 TeV [11, 12, 20].

Likelihood reconstructions are performed on every event in the final sample, simultaneously fitting a cascade hypothesis for deposited energy and vertex position and time. A vertex resolution of 9 m and an energy resolution of 0.12 in $\log_{10}$(E/GeV) are obtained. The absolute energy scale uncertainty is found to be 0.1 in $\log_{10}$(E/GeV). Using the energy reconstruction in Fig. 3 (rebinned to get sufficient statistics and reasonable uncertainties in each bin), we subtract the atmospheric muon and the atmospheric ν_μ CC and ν_μ NC to estimate the ν_e excess. The ν_e excess is converted into flux by normal-

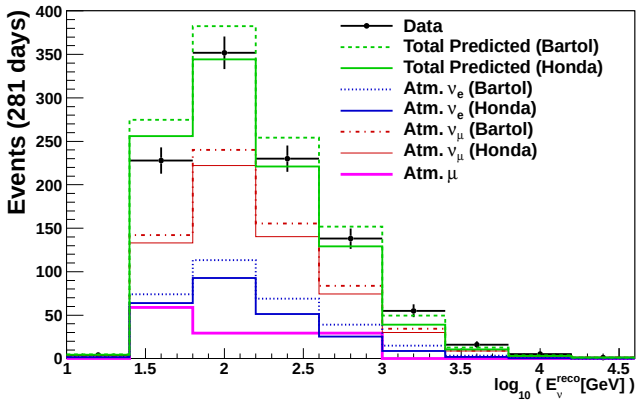

FIG. 3. (Color online) The event rate as a function of the reconstructed cascade energy. The sum of all MC expectations (green) is consistent with 281 days of data rate. The dotted lines show the Bartol prediction while the solid lines indicate Honda predictions for the atmospheric neutrinos. Systematic uncertainties (Table II) are omitted for clarity.

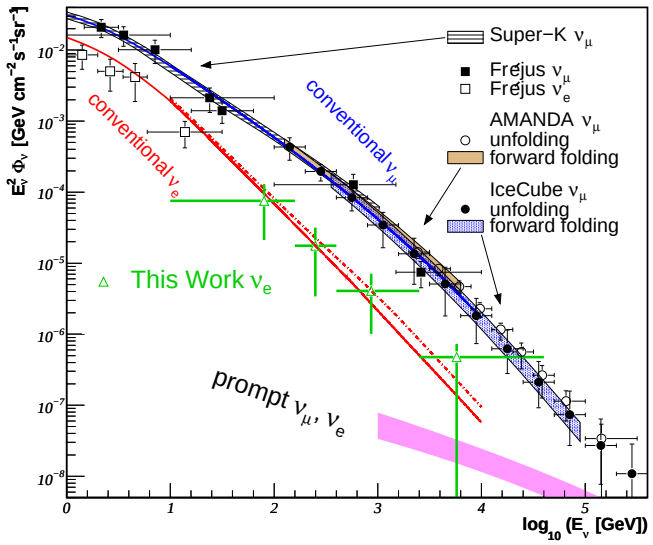

FIG. 4. (Color online) The electron neutrino spectrum (green open triangles). The conventional ν_e (red line) and ν_μ (blue line) from Honda, ν_e (red dotted line) from Bartol and charm-induced neutrinos (magenta band) [29] are shown. Previous measurements from Super-K [30], Fréjus [4], AMANDA [31, 32] and IceCube [1, 33] are also shown.

TABLE III. The $E_\nu^2\Phi_\nu$ flux. E_ν is in GeV.

$\log_{10}E_\nu^{\rm min} - \log_{10}E_\nu^{\rm max}$	$\langle E_\nu \rangle$	$E_\nu^2\Phi_\nu$(GeV cm^{-2}s^{-1}sr^{-1})
1.0 − 2.2	80	$(7.5 \pm 5.4) \times 10^{-5}$
2.2 − 2.6	251	$(1.8 \pm 1.4) \times 10^{-5}$
2.6 − 3.4	865	$(4.1 \pm 3.1) \times 10^{-6}$
3.4 − 4.6	5753	$4.8^{+2.6}_{-4.8} \times 10^{-7}$

izing to the expected number of events from an average of the Bartol and Honda fluxes. In each bin, the horizontal bar indicates the bin width. The marker placement shows the average reconstructed energy of the contributing events. The vertical error bars include the statistical and systematic uncertainties (see Fig. 4 and Table III).

In conclusion, we have observed atmospheric neutrino-induced cascades, produced by ν_e CC interactions and NC interactions of all flavors in IceCube. The atmospheric ν_e flux in the energy range between 80 GeV and 6 TeV is consistent with current models of the atmospheric neutrino flux. More sophisticated event reconstruction algorithms now in development, combined with the additional information from the final two DeepCore strings deployed in late 2010, should provide substantially improved discrimination against the ν_μ CC background. This will provide both a more precise measurement of the electron neutrino flux and a reduced energy threshold, enabling observation of oscillation phenomena in the cascade channel.

We acknowledge the support from the following agencies: U.S. National Science Foundation-Office of Polar Programs, U.S. National Science Foundation-Physics Division, University of Wisconsin Alumni Research Foundation, the Grid Laboratory Of Wisconsin (GLOW) grid infrastructure at the University of Wisconsin - Madison, the Open Science Grid (OSG) grid infrastructure; U.S. Department of Energy, and National Energy Research Scientific Computing Center, the Louisiana Optical Network Initiative (LONI) grid computing resources; National Science and Engineering Research Council of Canada; Swedish Research Council, Swedish Polar Research Secretariat, Swedish National Infrastructure for Computing (SNIC), and Knut and Alice Wallenberg Foundation, Sweden; German Ministry for Education and Research (BMBF), Deutsche Forschungsgemeinschaft (DFG), Helmholtz Alliance for Astroparticle Physics (HAP), Research Department of Plasmas with Complex Interactions (Bochum), Germany; Fund for Scientific Research (FNRS-FWO), FWO Odysseus programme, Flanders Institute to encourage scientific and technological research in industry (IWT), Belgian Federal Science Policy Office (Belspo); University of Oxford, United Kingdom; Marsden Fund, New Zealand; Australian Research Council; Japan Society for Promotion of Science (JSPS); the Swiss National Science Foundation (SNSF), Switzerland.

* Physics Department, South Dakota School of Mines and Technology, Rapid City, SD 57701, USA
† Corresponding authors.
‡ Los Alamos National Laboratory, Los Alamos, NM 87545, USA
§ also Sezione INFN, Dipartimento di Fisica, I-70126, Bari, Italy
¶ NASA Goddard Space Flight Center, Greenbelt, MD 20771, USA

[1] R. Abbasi *et al.* (IceCube Collaboration), Phys. Rev. D **83**, 012001 (2011).
[2] R. Becker-Szendy *et al.* (IMB-3 Collaboration), Phys. Rev. D **46**, 3720 (1992).
[3] R. Wendell *et al.* (Super-Kamiokande Collaboration), Phys. Rev. D **81**, 092004 (2010).
[4] K. Daum *et al.* (Fréjus Collaboration), Z. Phys. C **66**, 417 (1995).
[5] M. Aglietta *et al.* (NUSEX Collaboration), Europhys. Lett. **8**, 611 (1989).
[6] M. Sanchez *et al.* (Soudan-2 Collaboration), Phys. Rev. D **68**, 113004 (2003).
[7] M. Ackermann *et al.* (AMANDA Collaboration), Astropart. Phys. **22**, 127 (2004).
[8] R. Abbasi *et al.* (IceCube Collaboration), Astropart. Phys. **34**, 420 (2011).
[9] R. Abbasi *et al.* (IceCube Collaboration), Phys. Rev. D **84**, 072001 (2011).
[10] R. Abbasi *et al.* (IceCube Collaboration), in *Proc. of 32nd ICRC, Beijing, China* (2011) arXiv:1111.2736.
[11] M. Honda, T. Kajita, K. Kasahara, S. Midorikawa, and T. Sanuki, Phys. Rev. D **75**, 043006 (2007).
[12] G. D. Barr, S. Robbins, T. K. Gaisser, and T. Stanev, Phys. Rev. D **74**, 094009 (2006).
[13] D. J. Koskinen, Mod. Phys. Lett. **A26**, 2899 (2011).

[14] G. Giordano, O. Mena, and I. Mocioiu, Phys. Rev. D **81**, 113008 (2010).
[15] R. Abbasi *et al.* (IceCube Collaboration), Astropart. Phys. **35**, 615 (2012).
[16] R. Abbasi *et al.* (IceCube Collaboration), Nucl. Instrum. Meth. **A618**, 139 (2010).
[17] R. Abbasi *et al.* (IceCube Collaboration), Nucl. Instrum. Meth. **A601**, 294 (2009).
[18] D. Heck *et al.*, Tech. Rep. FZKA **6019**, 1 (1998).
[19] A. Gazizov and M. P. Kowalski, Comput. Phys. Commun. **172**, 203 (2005).
[20] G. D. Barr, T. K. Gaisser, P. Lipari, S. Robbins, and T. Stanev, Phys. Rev. D **70**, 023006 (2004).
[21] A. Hocker, J. Stelzer, F. Tegenfeldt, H. Voss, K. Voss, *et al.*, PoS **ACAT**, 040 (2007).
[22] J. Ahrens *et al.* (AMANDA Collaboration), Nucl. Instrum. Meth. **A524**, 169 (2004).
[23] C. Ha, Ph.D. dissertation, Pennsylvania State University https://etda.libraries.psu.edu/paper/12119 (2011).
[24] M. Ackermann *et al.* (The IceCube Collaboration), J. Geophys. Res. **111**, D13203 (2006).
[25] M. Aartsen *et al.* (IceCube Collaboration), Nucl. Instrum. Meth. **A711**, 73 (2013).
[26] J. R. Hoerandel, Astropart. Phys. **19**, 193 (2003).
[27] M. Gonzalez-Garcia, M. Maltoni, and J. Salvado, JHEP **1004**, 056 (2010).
[28] T. Sanuki, M. Honda, T. Kajita, K. Kasahara, and S. Midorikawa, Phys. Rev. D **75**, 043005 (2007).
[29] R. Enberg, M. H. Reno, and I. Sarcevic, Phys. Rev. D **78**, 043005 (2008).
[30] M. Gonzalez-Garcia, M. Maltoni, and J. Rojo, JHEP **0610**, 075 (2006).
[31] R. Abbasi *et al.* (IceCube Collaboration), Phys. Rev. D **79**, 102005 (2009).
[32] R. Abbasi *et al.* (IceCube Collaboration), Astropart. Phys. **34**, 48 (2010).
[33] R. Abbasi *et al.* (IceCube Collaboration), Phys. Rev. D **84**, 082001 (2011).